Article

Electron Capture Dissociation Initiates a Free Radical Reaction Cascade

Nancy Leymarie, Catherine E. Costello, and Peter B. O'Connor

J. Am. Chem. Soc., **2003**, 125 (29), 8949-8958• DOI: 10.1021/ja028831n • Publication Date (Web): 01 July 2003

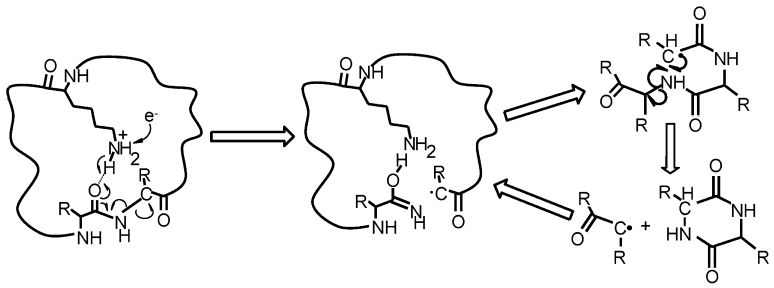

More About This Article

Additional resources and features associated with this article are available within the HTML version:

- Supporting Information
- Links to the 11 articles that cite this article, as of the time of this article download
- Access to high resolution figures
- Links to articles and content related to this article
- Copyright permission to reproduce figures and/or text from this article

View the Full Text HTML

J|A|C|S
ARTICLES
Published on Web 07/01/2003

Electron Capture Dissociation Initiates a Free Radical Reaction Cascade

Nancy Leymarie, Catherine E. Costello, and Peter B. O'Connor*

Contribution from the Mass Spectrometry Resource, Department of Biochemistry, Boston University School of Medicine, 715 Albany Street, R806, Boston, Massachusetts 02118

Received October 5, 2002; E-mail: poconnor@bu.edu

Abstract: For small cyclic peptides, one electron capture by the $[M + 2H]^{2+}$ ion generates numerous fragments corresponding to amino acid losses, side-chain losses, and losses of some low molecular weight species such as H_2O, $CH_3^{\bullet}$, C_3H_6, and $^{\bullet}CONH_2$. As predicted, the side-chain cleavages are amplified relative to linear peptides of similar size, but the amino acid losses were unexpected because they require that one electron capture cause more than one backbone cleavage, a phenomenon which necessitates further refinement or reinterpretation of current ECD mechanisms. A modified mechanism is postulated in which nonergodic electron capture fragmentation generates an α-carbon radical species that then propagates along the protein backbone. This radical migration initiates multiple free radical rearrangements, which cause both multiple backbone cleavages and additional side-chain cleavages.

Introduction

The reactions of protein radicals[1−4] are highly complex, involving numerous rearrangements, many of which have extremely low (or zero) activation barriers.[5−7] Such free radical rearrangements give rise to protein cleavage, side-chain losses, and disulfide preferential reactions, among others.[8] These reactions are numerous and show relatively low selectivity as many of the various reaction channels differ only slightly in the reaction energetics. While much of what is known about the mechanisms of protein radical reactions derives from solution phase chemistry, they provide an interesting comparison system for the unusual reactions that have been observed for protein free radicals in the gas phase.

Gas-phase reaction of low energy electrons with multiply charged polypeptide and protein molecular ions (electron capture dissociation, ECD)[9,10] in the Fourier transform mass spectrometer (FTMS)[11] shows intriguing new capabilities for the analysis of protein structure, including the ability to cleave a protein's backbone while leaving intact labile side-chain modifications,[12] such as phosphorylation[13] or *N*-[14] and *O*-linked[15] glycosylation. The primary mechanism[9] (eq 1) involves neutralization of a hydrogen bonded amine with transfer of the $H^{\bullet}$ to the backbone carbonyl, cleaving the backbone $N-C_\alpha$ bond and forming a radical on the α-carbon. Gas-phase carbon radicals are well known for being extremely reactive[16] so that secondary fragmentation is likely, a hypothesis that is straightforward to test using doubly charged cyclic peptides.

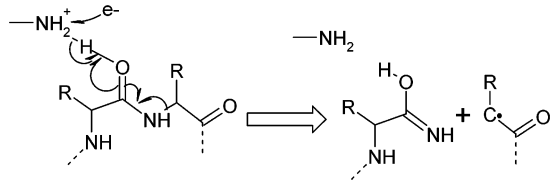

Recent results have shown the ability to cleave the protein backbone without disrupting the noncovalent associations that

(1) Dean, R. T.; Fu, S.; Stocker, R.; Davies, M. J. Biochemistry and pathology of radical-mediated protein oxidation. *Biochem. J.* **1997**, *324*, 1−18.
(2) Turecek, F.; Carpenter, F. H. Glycine radicals in the gas phase. *J. Chem. Soc., Perkin Trans. 2* **1999**, 2315−2323.
(3) Syrstad, E. A.; Stephens, D. D.; Turecek, F. Hydrogen atom adducts to the amide bond. Generation and energetics of amide radicals in the gas phase. *J. Phys. Chem. A* **2003**, *107*, 115−126.
(4) Turecek, F.; Syrstad, E. A. Mechanism and energetics of intramolecular hydrogen transfer in amide and peptide radicals and cation-radicals. *J. Am. Chem. Soc.* **2003**, *125*, 3353−3369.
(5) Rauk, A.; Yu, D.; Armstrong, D. A. Oxidative damage to and by cysteine in proteins: An ab initio study of the radical structures, C−H, S−H, and C−C bond dissociation energies, and transition structures for H abstraction by thiyl radicals. *J. Am. Chem. Soc.* **1998**, *120*, 8848−8855.
(6) Rauk, A.; Yu, D.; Armstrong, D. A. Toward site specificity of oxidative damage in proteins: C−H and C−C bond dissociation energies and reduction potentials of the radicals of alanine, serine, and threonine residues − an ab initio study. *J. Am. Chem. Soc.* **1997**, *119*, 208−217.
(7) Rauk, A.; Yu, D.; Taylor, J.; Shustov, G. V.; Block, D. A.; Armstrong, D. A. Effects of structure on α C−H bond enthalpies of amino acid residues: Relevance to H transfers in enzyme mechanisms and in protein oxidation. *Biochemistry* **1999**, *38*, 9089−9096.
(8) Hawkins, C. L.; Davies, M. J. Generation and propagation of radical reactions on proteins. *Biochim. Biophys. Acta* **2001**, *1504*, 196−219.
(9) Zubarev, R. A.; Kelleher, N. L.; McLafferty, F. W. Electron capture dissociation of multiply charged protein cations − a nonergodic process. *J. Am. Chem. Soc.* **1998**, *120*, 3265−3266.
(10) McLafferty, F. W.; Horn, D. M.; Breuker, K.; Ge, Y.; Lewis, M. A.; Cerda, B.; Zubarev, R. A.; Carpenter, B. K. Electron capture dissociation of gaseous multiply charged ions by Fourier-transform ion cyclotron resonance. *J. Am. Soc. Mass Spectrom.* **2001**, *12*, 245−249.
(11) Marshall, A. G.; Hendrickson, C. L.; Jackson, G. S. Fourier transform ion cyclotron resonance mass spectrometry − a primer. *Mass Spectrom. Rev.* **1998**, *17*, 1−35.
(12) Kelleher, R. L.; Zubarev, R. A.; Bush, K.; Furie, B.; Furie, B. C.; McLafferty, F. W.; Walsh, C. T. Localization of labile posttranslational modifications by electron capture dissociation: The case of γ-carboxyglutamic acid. *Anal. Chem.* **1999**, *71*, 4250−4253.
(13) Shi, S. D. H.; Hemling, M. E.; Carr, S. A.; Horn, D. M.; Lindh, I.; McLafferty, F. W. Phosphopeptide/phosphoprotein mapping by electron capture dissociation mass spectrometry. *Anal. Chem.* **2001**, *73*, 19−22.
(14) Hakansson, K.; Cooper, H. J.; Emmett, M. R.; Costello, C. E.; Marshall, A. G.; Nilsson, C. L. Electron capture dissociation and infrared multiphoton dissociation MS/MS of an N-glycosylated tryptic peptide to yield complementary sequence information. *Anal. Chem.* **2001**, *73*, 4530−4536.

determine a protein's three-dimensional structure.[17,18] Additionally, some side-chain cleavages of proteins have been observed for ECD[9,19] and are useful in distinguishing Leu/Ile isomers.[20,21] The combination of nonergodic backbone fragmentation and structurally diagnostic side-chain cleavages offers potentially interesting new capabilities in the analysis of posttranslationally modified proteins.

Results from Zubarev et al. suggest that ECD proceeds via a nonergodic dissociation mechanism[9] due to the fact that the Coulombic recombination energy is simply insufficient to cause any kind of fragmentation if the energy is distributed into the $3N - 6$ normal modes of the molecule. To explain the relative nonselectivity of ECD (with the notable exception of proline)[22] when compared to collisional activation methods[23] and the relative abundance of cleavages at S−S bonds, a model was proposed in which the H$^{\bullet}$ released by electron capture became mobile within the protein prior to cleavage.[24,25] The mobile H$^{\bullet}$ would then react (per eq 1) to cause cleavage at many points statistically distributed throughout the protein. With this model, one electron generates one H$^{\bullet}$ resulting in one cleavage, but secondary fragmentation is not common.

To further test this model as well as to further explore reported[19,20] side-chain cleavages generated by ECD, doubly charged cyclic peptides were subjected to electron capture dissociation with the premise that backbone fragmentation of linear peptides or side-chain cleavages require one electron capture and one cleavage, but formation of fragment ions from cleavage of the backbone of a cyclic peptide would require capture of two electrons, reducing the charge state of backbone fragments to zero and rendering them undetectable. Thus, the abundance of ions corresponding to side-chain cleavage reactions would effectively be amplified as compared to backbone cleavages. Although the premise of amplification of side-chain cleavages was verified by the experiment, additional unexpected fragments were also observed. The data presented in this paper demonstrate that extensive secondary backbone bond cleavages follow a single electron capture. We postulate a mechanism involving a cascade of free radical reactions to explain these results.

Experimental Section

The mass spectrometer used was a previously described[22] electrospray ionization Fourier transform mass spectrometer. The cyclic peptides were purchased from Sigma-Aldrich (St. Louis, MO), except for the gramicidin *S* which was a kind gift from Prof. Vouros. The peptides were dissolved to ~1 pmol/μL in 50:50:1 H_2O:CH_3OH:formic acid, and ~1−5 μL was used in pulled glass capillary nanospray tips[26] to generate multiply charged ions. The low energy electrons needed for ECD were generated by two methods, a heated tungsten filament (resistively heated with 1 V and 2.6 A), and an indirectly heated dispenser cathode[27] (model STD200, Heatwave, Watsonville, CA, heated with 5 V and 1.1 A). The center potential of the filament and the dispenser cathode were both biased at −0.2 V relative to ground, with the outer trapping plates held at +10 V, and the inner trapping ring held at +1 V during ECD. The gramicidin *S* spectrum used a Nyquist frequency of 1 MHz that corresponded to a low mass limit, ~*m*/*z* 108; the LLFHWAVGH and cyclosporin *A* spectra were detected with a Nyquist frequency of 500 kHz which corresponded to a low mass limit, ~*m*/*z* 215.

The spectra were acquired, zerofilled twice, and Fourier transformed without apodization. They were internally calibrated on the $[M + 2H]^{2+}$ and $[M + H]^{+}$ peaks and their isotopes, but even without internal calibration, the difference masses were usually within 5−10 ppm for a good assignment, and larger differences indicated a suspicious assignment. In an effort to assign as many peaks as possible, the mass tables (Tables 2−4) were created manually with the criteria that a peak had to be of sufficient signal/noise ratio that its isotopes could be detected and its mass defect was required to be reasonable for peptides. Foldback peaks, harmonics, noise spikes, and bleedthrough from the isolation waveform were not included. Isotopes were not included in the data tables unless the isotope pattern suggested that more than one component was present in the isotopic cluster. All masses represent monoisotopic peaks. All structures that are reported are assigned within a mass error of at most 0.015 Da unless otherwise noted. This mass difference corresponds to ~10−15 ppm at the molecular ion mass and thus represents a fairly broad acceptance window as compared to the (<5 ppm) mass accuracy of the instrument. Many of the assigned masses correspond to more than one possible structure within 0.015 Da, and the multiple assignments of each of these structures are listed in the tables. Table 1 shows mass losses observed for each cyclopeptide, and Tables 2−4 show the detailed assignments of all peaks observed for each cyclopeptide.

Results

The first spectrum (Figure 1a), from the peptide cyclo-LLFHWAVGH (Figure 2a), is a typical spectrum resulting from ECD of a doubly charged cyclic peptide. The mass losses can be roughly classified into three categories: small molecule losses, amino acid residue losses, and side-chain losses; these mass losses are reported in Table 1, and the complete peak list from the cyclo-LLFHWAVGH cyclopeptide spectrum is in Table 2. Although greater than 80% of the mass losses observed correspond to a combination of these losses, several as yet

(15) Mirgorodskaya, E.; Roepstorff, P.; Zubarev, R. A. Localization of O-glycosylation sites in peptides by electron capture dissociation in a Fourier transform mass spectrometer. *Anal. Chem.* **1999**, *71*, 4431−4436.
(16) McLafferty, F. W.; Turecek, F. *Interpretation of Mass Spectra*, 4th ed.; University Science Books: Mill Valley, CA, 1993.
(17) Horn, D. M.; Ge, Y.; McLafferty, F. W. Activated ion electron capture dissociation for mass spectral sequencing of larger (42 kDa) proteins. *Anal. Chem.* **2000**, *72*, 4778−4784.
(18) Breuker, K.; Oh, H.; Horn, D. M.; Cerda, B. A.; McLafferty, F. W. Detailed unfolding and folding of gaseous ubiquitin ions characterized by electron capture dissociation. *J. Am. Chem. Soc.* **2002**, *124*, 6407−6420.
(19) Cooper, H. J.; Hudgins, R. R.; Hakansson, K.; Marshall, A. G. Characterization of amino acid side chain losses in electron capture dissociation. *J. Am. Soc. Mass Spectrom.* **2002**, *13*, 241−249.
(20) Kjeldsen, F.; Haselmann, K. F.; Budnik, B. A.; Jensen, F.; Zubarev, R. A. Dissociative capture of hot (3−13 ev) electrons by polypeptide polycations: An efficient process accompanied by secondary fragmentation. *Chem. Phys. Lett.* **2002**, *356*, 201−206.
(21) Kjeldsen, F.; Haselmann, K. F.; Sorensen, E. S.; Zubarev, R. A. Distinguishing of Ile/Leu amino acid residues in the PP3 protein by (hot) electron capture dissociation in Fourier transform ion cyclotron resonance mass spectrometry. *Anal. Chem.* **2003**, *75*, 1267−1274.
(22) Leymarie, N.; Berg, E. A.; McComb, M. E.; O'Connor, P. B.; Grogan, J.; Oppenheim, F. G.; Costello, C. E. Tandem mass spectrometry for structural characterization of proline-rich proteins: Application to salivary PRP-3. *Anal. Chem.* **2002**, *74*, 4124−4132.
(23) Kruger, N. A.; Zubarev, R. A.; Carpenter, B. K.; Kelleher, N. L.; Horn, D. M.; McLafferty, F. W. Electron capture versus energetic dissociation of protein ions. *Int. J. Mass Spectrom. Ion Processes* **1999**, *183*, 1−5.
(24) Zubarev, R. A.; Kruger, N. A.; Fridriksson, E. K.; Lewis, M. A.; Horn, D. M.; Carpenter, B. K.; McLafferty, F. W. Electron capture dissociation of gaseous multiply charged proteins is favored at disulfide bonds and other sites of high hydrogen atom affinity. *J. Am. Chem. Soc.* **1999**, *121*, 2857−2862.
(25) Zubarev, R. A.; Haselmann, K. F.; Budnik, B.; Kjeldsen, F.; Jensen, F. Towards an understanding of the mechanism of electron-capture dissociation: A historical perspective and modern ideas. *Eur. J. Mass Spectrom.* **2002**, *8*, 337−349.
(26) Valaskovic, G. A.; Kelleher, N. L.; Little, D. P.; Aaserud, D. J.; McLafferty, F. W. Attomole-sensitivity electrospray source for large-molecule mass spectrometry. *Anal. Chem.* **1995**, *67*, 3802−3805.
(27) Tsybin, Y. O.; Hakansson, P.; Budnik, B. A.; Haselmann, K. F.; Kjeldsen, F.; Gorshkov, M.; Zubarev, R. A. Improved low-energy electron injection systems for high rate electron capture dissociation in Fourier transform ion cyclotron resonance mass spectrometry. *Rapid Commun. Mass Spectrom.* **2001**, *15*, 1849−1854.

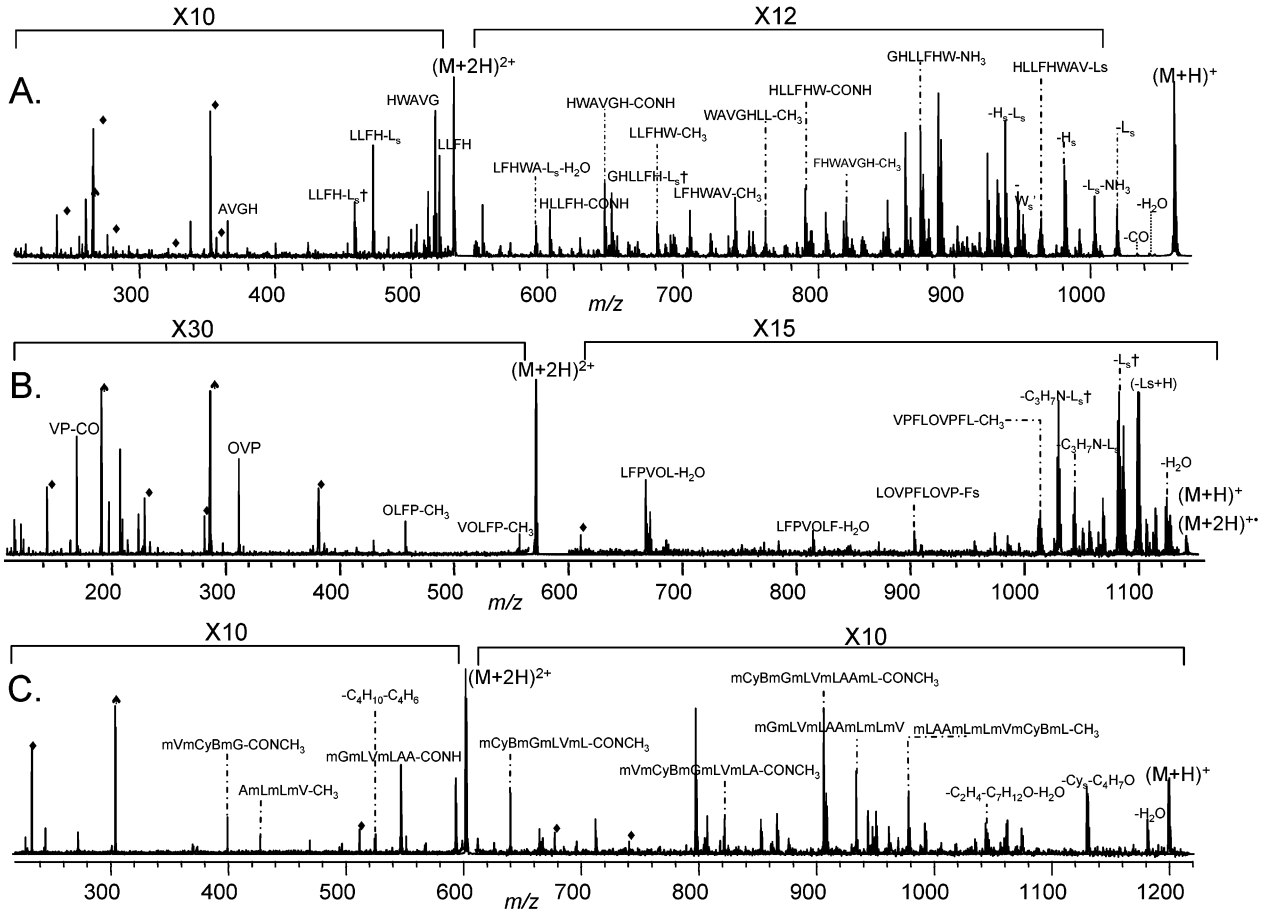

Figure 1. Electron capture dissociation mass spectra of the $[M + 2H]^{2+}$ ions of (A) the cyclopeptide cyclo-LLFHWAVGH, (B) gramicidin *S*, and (C) cyclosporin *A*.

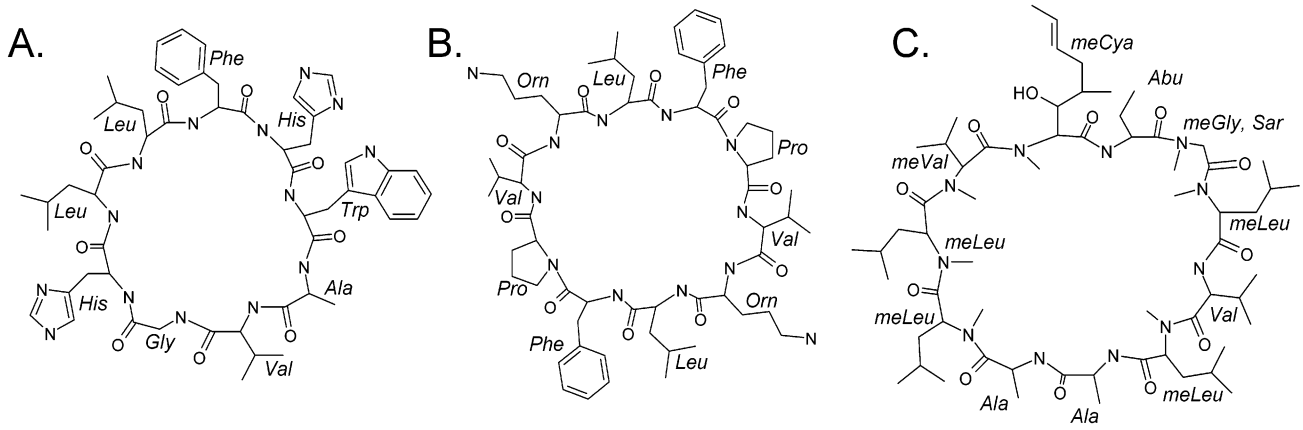

Figure 2. Cyclic peptide structures of (A) the cyclopeptide cyclo-LLFHWAVGH, (B) gramicidin *S*, and (C) cyclosporin *A*.

unidentified peaks exist. Particular small molecule and radical losses are abundant including elimination of H• (1.0078 Da), CH_3• (15.023 Da), H_2 (2.014 Da), H_2O (18.011 Da), •$CONH_2$ (44.014 Da), C_3H_6 (42.047 Da), and C_3H_7• (43.055 Da). Backbone cleavage is common and can be observed in the intense peaks corresponding to losses of tryptophan, histidine, alanine, and valine from the molecular ion and the less abundant losses corresponding to each of the other amino acid residues in the sequence. Not all side-chain cleavages are apparent, but several previously unreported side-chain cleavages are observed in this spectrum. Even-electron side-chain losses of tryptophan (C_9H_8N, 130.065 Da), histidine (82.054 Da), phenylalanine (C_7H_8, 92.063 Da), and valine (C_3H_6, 42.047 Da) are evident as well as radical side-chain losses for valine (C_3H_7•, 43.055 Da), alanine (CH_3•, 15.023 Da), glycine (H•, 1.0078 Da), and tryptophan (C_8H_6N•, 116.050 Da). Some of these losses have multiple possible explanations; for example, the C_3H_7• or CH_3• losses could in some cases also be attributed to a w-28 ion from leucine or valine, respectively. Many of the observed mass losses

(28) For peptide ion fragmentation nomenclature, see: (a) Roepstorff, P.; Fohlman, J. Proposal for a common nomenclature for sequence ions in mass spectra of peptides. *Biomed. Mass Spectrom.* **1984**, *11*, 601. As modified by: (b) Biemann, K. Contributions of mass spectrometry to peptide and protein structure. *Biomed. Environ. Mass Spectrom.* **1988**, *16*, 99−111.

Table 1. Losses Noted for Each Cyclic Peptide[a]

	cyclo-LLFHWAVGH	gramicidin *S*	cyclosporin *A*
small molecule losses	$H^{\bullet}$, $CH_3^{\bullet}$, H_2, H_2O, HCN, CO, CHON,	$H^{\bullet}$, $CH_3^{\bullet}$, CH_4, H_2, H_2O, CO, CHON, C_2H_6, NH_3, C_4H_8, C_3H_8, $CH_4N^{\bullet}$	$H^{\bullet}$, $CH_3^{\bullet}$, CH_4, H_2O, CO, CHON, $CONCH_3$,
amino acid losses	1°: Trp, His, Val/Leu, Ala	1°: Orn, Phe, Val/Leu,	1°: MeVal, MeGly, Abu, MeCy, Val/Leu, MeLeu
	2°: all amino acids in peptide	2°: all amino acids in peptide	2°: all amino acids in peptide
side chain losses	Trp ($C_9H_8N^{\bullet}$, $C_8H_6N^{\bullet}$), His ($C_4H_6N_2$), Phe (C_7H_8, $C_6H_5^{\bullet}$), Val/Leu (C_3H_6, $C_3H_7^{\bullet}$)	Orn ($C_2H_6N^{\bullet}$, $C_3H_7N^{\bullet}$), Phe (C_7H_8, $C_6H_5^{\bullet}$), Val/Leu (C_3H_6, $C_3H_7^{\bullet}$)	MeCy ($C_4H_7O^{\bullet}$, C_2H_4O), Val/Leu (C_3H_6, $C_3H_7^{\bullet}$)

[a] 1° amino acid losses refers to losses observed directly from the molecular ion, and 2° amino acid losses refer to losses from a smaller molecular weight species.

correspond to a sum of even-electron losses so that the radical site must remain on the charge-containing peptide (a phenomenon which is commonly observed for gas-phase radical ions),[16] and furthermore no cases are apparent that correspond to the elimination of two known radical species. Finally, multiple backbone cleavages result in peaks that correspond to a series of sequential amino acid losses so that the same backbone bond must be cleaved on each end of the peptide.

Gramicidin *S* (Figure 2b) is a repetitive cyclic peptide with the sequence cyclo-VOLFPVOLFP and shows a spectrum (Figure 1b, Table 3) very similar to that of cyclo-LLFHWAVGH. Prior EIEIO[29] spectra of gramicidin *S*[30] showed similar complexity, but, at the time, few of the peaks could be assigned. In this case, the small molecule losses were similar to those above, but with the addition of C_2H_6, CO, and C_3H_8. All amino acid mass differences were detectable except proline. Because of its cyclic structure, observation of side-chain losses for proline would require two cleavages, making it less likely. Furthermore, likely proline side-chain cleavages could correspond to $C_3H_7^{\bullet}$ (observed), C_3H_6 (observed), and C_3H_8 (observed, but unlikely to be formed from proline as it would require two $H^{\bullet}$ transfers), but as all three of these mass losses could also be formed from valine or leucine (processes which are much more likely), side-chain losses for proline cannot be specified from these data. Finally, as observed above, sequential fragments whose losses correspond to the masses of adjacent amino acid residues in the sequence are also seen in the mass spectrum of gramicidin *S*.

The ECD mass spectrum of cyclosporin *A* (Figure 1c, Table 4) shows some differences from the other cyclic peptides, but this is expected, as the structure of cyclosporin *A* (Figure 2c) varies strongly from that of a traditional cyclic peptide, in that all but four of the amino acids are N-methylated and two unusual amino acids are present, aminobutyric acid (Abu or B) and $-N(CH_3)CH(CH(OH)CH(CH_3)CH_2CH{=}CHCH_3)CO-$ (denoted mCy). Additionally, there are no side chains capable of forming a protonated amine so that the most likely charge sites are the backbone amide bonds. This spectrum, overall, contains fewer peaks than the spectra of the previous two cyclopeptides and is more prone to the ± 1.0078 Da difference observed between parallel eliminations occurring as an even-electron or as an odd-electron species; this spectral feature has interesting implications which are discussed below. As above, small molecule and radical losses are common and correspond to elimination of $H^{\bullet}$, H_2O, C_3H_6, $C_3H_7^{\bullet}$, HCN, and CHON. In addition, losses of C_4H_6O and C_2H_4O are apparent. $CH_3^{\bullet}$ losses are observed less frequently than are CH_4 losses. Elimination of the whole amino acid residues of mVal, mGly (or Sarcosine, Sar), Abu, mCy, Val, and mLeu are observed, but only as secondary fragment ions. Side-chain cleavages from Val/Leu (C_3H_6, $C_3H_7^{\bullet}$) and mCy are visible. Series of losses corresponding to sequential amino acid residues are observed as before. The most likely charge sites on cyclosporin *A* are the backbone N-methyl amides, so it is not surprising that all of the observed fragments include at least one of these sites.

Discussion

Electron capture dissociation mass spectra indicate that these small doubly charged cyclic peptides are much more prone to $H^{\bullet}$ loss than are larger proteins.[9,24,31] In fact, only the cyclosporin *A* yielded a detectable $[M + 2H]^{+\bullet}$ peak, and cyclosporin *A* generated many more fragment ion peaks that correspond to a stabilized radical species (see below), as compared to cyclic LLFHWAVGR and gramicidin *S*. This increased probability of $H^{\bullet}$ loss on the small cyclic peptides can be explained by the competition between $H^{\bullet}$ loss and backbone cleavage. Because two backbone cleavages are required to generate a larger mass loss versus a single cleavage to eliminate $H^{\bullet}$, increased $H^{\bullet}$ loss would be expected. The stability of the radical generated from cyclosporin *A* is discussed below.

Cyclic Peptides. Tandem mass spectrometry of cyclic peptides typically generates extremely complex spectra due to the initial ring-opening fragmentation being statistically distributed around the peptide, with subsequent fragments generated from this statistical mixture.[32] Not surprisingly, this complexity is also apparent in the ECD spectra of cyclic peptides. We attempted to use the cyclic peptide cleavage nomenclature introduced by Ngoka and Gross,[33] but this system of nomenclature is limited to describing peptides in which one of the two cleavages occurs at the amide bond. Because of the highly complex nature of these ECD spectra, it was found that this nomenclature system was not sufficient, and thus the fragments are described in the simplest way possible, as a base composition of amino acids with a fragment loss from that base.

(29) Cody, R. B.; Freiser, B. S. Electron impact excitation of ions in Fourier transform mass spectrometry. *Anal. Chem.* **1987**, *59*, 1054−1056.
(30) Wang, B.-H.; McLafferty, F. W. Electron impact excitation of ions from larger organic molecules. *Org. Mass Spectrom.* **1990**, *25*, 554−556.
(31) Breuker, K.; Oh, H. B.; Cerda, B.; Horn, D.; Mclafferty, F. W. Hydrogen atom loss in electron-capture dissociation: A Fourier transform-ion cyclotron resonance study with single isotopomeric ubiquitin ions. *Eur. J. Mass Spectrom.* **2002**, *8*, 177−180.
(32) Eckart, K. Mass spectrometry of cyclic peptides. *J. Mass Spectrom.* **1994**, *13*, 23−55.
(33) Ngoka, L. C. M.; Gross, M. L. A nomenclature system for labeling cyclic peptide fragments. *J. Am. Soc. Mass Spectom.* **1999**, *10*, 360−363.

Table 2. Cyclopeptide cyclo-FHWAVGHLL $[M + 2H]^{2+}$ ECD Fragment Table

base	fragment	measured masses	calculated masses	base	fragment	measured masses	calculated masses
FHWAVGHLL	$[M + H]^+$	1061.5674	1061.5685(1.0)	FHWAVGH	$-(CONH + H^\bullet)$	792.3938	792.3945(0.9)
FHWAVGHLL	$-(CH_3 + H^\bullet)$	1047.5485	1047.5534(4.7)	HLLFHW	$-(CONH + H^\bullet)$	791.4380	791.4357(2.9)
FHWAVGHLL	$-(H_2O + H^\bullet)$	1043.5567	1043.5575(7.7)	LLFHWAVG	$-(C_4H_6N_2 + H^\bullet)$	785.4459	785.4381(9.9)
FHWAVGHLL	$-(CO + H^\bullet)$	1034.5828	1034.5814(1.4)	WAVGHLL	$([M + H]^+)$	778.4473	778.4488(1.9)
FHWAVGHLL	$-(C_3H_6)$	1019.5214	1019.5218(0.4)	LLFHWAV	$-(C_7H_8)$	776.4227	776.4333(13.6)
FHWAVGHLL	$-(CONH + H^\bullet)$	1018.5639	1018.5627(1.2)	LFHWAVG	$-(CONH + H^\bullet)$	768.4258	768.4197(7.9)
FHWAVGHLL	$-(C_4H_8)$	1006.5229	1006.5137(9.0)	WAVGHLL	$-(CH_3 + H^\bullet)$	762.4322	762.4182(18.4)
FHWAVGHLL	$-(C_3H_6 + NH_3)$	1002.4960	1002.4954(0.6)	VGHLLFH	$-(CONH + H^\bullet)$	761.4512	761.4462(6.6)
FHWAVGHLL	$-(C_3H_6 + H_2O)$	1001.5088	1001.5108(2.0)		unidentified	753.4153	
VGHLLFHW	$([M + H]^+)$	991.5253	991.5388(13.6)	HLLFHW	$-(C_4H_6N_2)$	753.4029	753.3993(4.8)
FHWAVGHLL	$-(C_4H_6N_2)$	980.5256	980.5263(0.7)	LLFHWA	$-(H_2O + H^\bullet)$	750.4089	750.4090(0.0)
FHWAVGHLL	$-(C_3H_6 + C_4H_8)$	963.4529	963.4592(6.5)	VGHLLFH	$-(C_4H_8)$	749.3919	749.3972(7.1)
GHLLFHWA	$[M + H]^+$	962.5003	962.5000(0.3)	LFHWAV	$-(CH_3)\ -(C_4H_6N_2 +$	740.3990	740.3889(13.6)
HLLFHWAA	$-(C_3H_6)$		962.5003(0.0)	HWAVGHLL	$C_7H_8 + H^\bullet)$		740.3874(15.7)
HLLFHWAA	$-(CONH + H^\bullet)$	961.5444	961.5412(3.3)	AVGHLLF	$([M + H]^+)$	739.4392	739.4378(1.8)
FHWAVGHLL	$-(2C_4H_8)$	950.4507	950.4511(0.4)	AVGHLLF	$[M + H]^+ -(C_9H_8N^\bullet)$	738.4252	738.4300(6.5)
FHWAVGHLL	$-(C_8H_6N^\bullet)$	946.5289	946.5264(2.6)	LLFHWAV	unidentified	735.3738	738.4356(14.1)
GHLLFHWA	$-(H_2O + H^\bullet)$	944.4984	944.4890(10.0)	AVGHLLF	$-(NH_3)$	722.4109	722.4115(0.8)
HLLFHWAV	$-(C_3H_6 + H_2O)$		944.4893(9.6)				
FHWAVGHLL	$-(C_4H_6N_2 + C_3H_6)$	937.4682	937.4718(3.8)		unidentified	707.4017	
FHWAVGHLL	$-(CONH + H^\bullet)$	936.5125	936.5127(0.2)	GHLLFH	$[M + H]^+$	705.3866	705.3840(3.7)
				HLLFH	$-(C_9H_8N^\bullet)$		705.3890(3.4)
FHWAVGHLL	$-(C_9H_8N^\bullet)$	932.5181	932.5160(2.3)	AVGHLLF	$-(C_3H_6)$	696.3861	696.3833(4.0)
				LFHWAVG	$-(C_8H_6N^\bullet)$		696.3828(4.6)
FHWAVGHLL	$-(C_9H_8N^\bullet + H^\bullet)$	931.5027	931.5082(5.9)	AVGHLLF	$-(CONH + H^\bullet)$	695.4257	695.4244(13.1)
	unidentified	929.5005		VGHLLFHW	$-(2C_4H_8)$	693.3381	693.3346(5.0)
				LFHWAV	$(C_3H_6 + H_2O)$		693.3385(0.6)
	unidentified	924.4607		HWAVGH	$([M + H]^+)$	689.3390	689.3397(10.4)
	unidentified	918.5370		FHWAVG	$-(CH_3)$	684.3305	684.3263(6.1)
HLLFHWAV	$-(C_7H_8)$	913.4940	913.4922(2.0)	AVGHLLFH	$-(C_4H_8 + H^\bullet)$	683.3788	683.3755(4.8)
VGHLLFHW	$-(C_4H_6N_2)$	909.4894	909.4892(0.1)		unidentified	669.3593	
LLFHWAVG	$-(CH_3 + H^\bullet)$		909.4866(3.1)				
WAVGHLLF	$-(CH_3 + H^\bullet)$						
FHWAVGHL	$-(C_3H_6)$	906.4371	906.4377(0.7)	GHLLFH	$-(CONH + H^\bullet)$	662.3744	662.3778(5.1)
GHLLFHWA	$-(C_4H_8 + H^\bullet)$		906.4374(3.3)				
HLLFHWAA	$-(C_3H_6 + C_4H_8)$		906.4377(0.7)				
LFHWAVGH	$-(C_3H_6)$		906.4373(0.2)				
FHWAVGHL	$-(CONH+ H^\bullet)$	905.4847	905.4786(6.7)	LLFHW	$-(CONH + H^\bullet)$	654.3791	654.3768(3.5)
LFHWAVG	unidentified	902.4653		VGHLLF	$-(H_2O)$	650.3799	650.3898(15.2)
HLLFHWA	$-(CH_3+ H^\bullet)$	890.4625	890.4457(7.6)	GHLLFH	$-(C_4H_8)$	650.3270	650.3288(2.8)
HLLFHWA	$-(CH_3 + H_2 + H^\bullet)$	888.4477	888.4400(8.7)		unidentified	648.3645	
WAVGHLLF	$-(CONH + H^\bullet)$	881.5047	881.5037(1.1)	HWAVGH	$-(CONH + H^\bullet)$	645.3289	645.3261(4.3)
LLFHWAVG				GHLLFH	$-(C_3H_6 + H_2O)$		645.3263(4.0)
GHLLFHWA	$-(H_2O)\ -(C_4H_6N_2 + C_3H_6)$	880.4446	880.4500(6.2)	AVGHLLF	$-(2 \times C_3H_6)$	627.3152	627.3126(4.1)
HLLFHWAV	unidentified	877.5103	880.4503(6.5)	HLLFH	$-(CONH + H^\bullet)$	605.3593	605.3564(4.8)
GHLLFHW	$-(CH_3)$	877.4542	877.4478(7.4)	LFHWA	$-(C_3H_6 + H_2O)$	595.2911	595.2783(21.5)
GHLLFHW	$-(NH_3)$	875.4431	875.444(1.3)	GHLLFH	$-(2C_4H_8)\ -(C_3H_6 +$	594.3225	594.2666(5.7)
				LFHWA	$H_2O + H^\bullet)$		594.2705(12.3)
	unidentified	868.3958			unidentified	594.2632	
GHLLFHW	$-(CO)$	864.4756	864.4758(0.2)	AVGHLL	$-(CH_3 + H^\bullet)$	576.3533	576.3389(25.0)
FHWAVGHLL	$-(C_4H_6N_2 + C_6H_5^\bullet)$		864.4763(0.6)				
LLFHWAV	$-(NH_3)$	851.4667	851.4694(3.2)	GHLLF	$([M + H]^+)$	569.3353	569.3328(3.9)
	unidentified	850.4600		AVGHLL	$[M + H]^+$	568.3286	568.3250(6.3)
				LLFHW	$-(C_9H_8N^\bullet)$		568.3301(2.6)
GHLLFHW	$-(CONH + H^\bullet)$	848.4551	848.4571(2.4)		unidentified	556.3280	
	unidentified	834.3948		HWAVG	$([M + H]^+)$	552.2821	552.2808(2.2)
				WAVGH			
	unidentified	833.3883		HWAVG	$[M + H]^+$	551.2762	551.2730(0.9)
				WAVGH			
AVGHLLFH	$-(CONH + H^\bullet)$	832.4924	832.4833(10.9)	FHWAV	$-(2 \times C_4H_8)$	516.2706	516.2642(12.4)
AVGHLLFH	$-(C_3H_6 + H^\bullet)$	832.4362	832.4346(1.9)		unidentified	513.3214	
AWHFLLHG	$-(C_9H_8N^\bullet + H^\bullet)$		832.4340(2.7)				
	unidentified	832.3838		HLLF LLFH	$([M + H]^+)$	512.3140	512.3108(0.4)
LLFHWAV	$-(C_3H_6)$	825.4407	825.4413(0.7)	HWAVG	$-(CONH + H^\bullet)$	508.2694	508.2672(4.3)
				WAVGH	$-(CONH + H^\bullet)$		508.2672(4.3)
				GHLLF	$-(C_3H_6 + H_2O)$		508.2673(4.2)
LLFHWAV	$-(CONH + H^\bullet)$	824.4841	824.4823(2.2)	FHWAV	$[M + H]^+$	500.2629	500.2537(18.4)
FHWAVGH	$-(CH_3)$	821.3937	821.3852(10.3)	FHWA	$-(CONH + H^\bullet)$	499.2594	499.2458(27.2)
FHWAVGH	$-(NH_3)$	819.3779	819.3816(4.5)		unidentified	496.2955	
FHWAVGH	$-(CO)$	808.4121	808.4132(1.4)	LLFH	$-(C_3H_6)$	469.2586	469.2563(4.7)
GHLLFHW	$-(C_4H_6N_2 + H_2)$		808.4185(3.3)	LFHW	$-(C_8H_6N^\bullet)$		469.2569(3.6)
LLFHWAV	$-(C_3H_6 + NH_3)$						
	unidentified	806.4698		LLFH	$-(C_4H_8)$	456.2515	456.2485(6.6)
	unidentified	796.4637		AVGH	$([M + H]^+)$	366.2036	366.2018 (2.2)
				GHLL	$-(C_4H_8)$		366.2015(5.7)
LFHWAVG	$-(NH_3)$	795.4029	795.4068(4.9)	LF	$-(NH_3)$	245.1414	245.1416(0.8)
	unidentified	794.3959					

[a] Masses are calculated as described in the text, mass errors (absolute value, ppm) between calculated and measured masses are noted in parentheses, and fragments are expressed relative to $[M + 2H]^{+\bullet}$. Note: Because these are cyclopeptides, masses are calculated as the sum of the amino acid residues masses (without the usual endgroups) minus the fragment. Note: A fragment key follows and also applies to Tables 3 and 4. Fragment mass key: Ls, C_3H_7 (43.0545); Ls′, C_3H_8 (44.0532); Ls†, C_4H_8 (56.0626); Ws, C_9H_8N (130.0656); Ws′, C_8H_6N (116.04995); Fs, C_7H_8 (92.0626); Fs′, C_7H_9 (93.0704); Fs†, C_6H_5 (77.039); Vs, C_3H_9N (59.0734); Hs, $C_4N_2H_6$ (82.05315); Cy(s), C_4H_7O (71.0497).

Table 3. Gramicidin *S* $[M + 2H]^{2+}$ ECD Fragment Table[a]

base	fragment	measured masses	calculated masses	base	fragment	measured masses	calculated masses
VOLFPVOLFP	$[M + 2H]^{+\bullet}$	1142.7176	1142.7176(0.0)	VOLFPVOLFP	$-(CH_3 + C_3H_7N + C_4H_8)$	1013.5726	1013.5699(2.7)
				OVPFLOVPF	$-NH$		1013.6149(1.3)
VOLFPVOLFP	$[M + H]^+$	1141.7132	1141.7137(0.4)	VOLFPVOLFP	$-(C_3H_7N + C_4H_8 + H_2O)$	1011.5869	1011.5902(3.3)
VOLFPVOLFP	$-H_2$	1139.7085	1139.7085(8.8)	VOLFPVOLFP	$-(C_7H_8 + C_4H_8)$	994.5908	994.5964(5.6)
VOLFPVOLFP	$-(CH_4 + H^\bullet)$	1127.6909	1127.6987(6.8)	VPFLOVPFL	$-(CONH + H^\bullet)$	984.6343	984.6286(5.8)
VOLFPVOLFP	$-H_2O$	1124.7081	1124.7106(2.1)	VOLFPVOLFP	$-(C_3H_7N + (2 \times C_4H_8))$	973.5439	973.5386(5.4)
VOLFPVOLFP	$-(H_2O + H^\bullet)$	1123.7047	1123.7027(1.8)	LOVPFLOVP	$-C_7H_8 - (CONH + H^\bullet)$	902.5853	902.5827(2.9)
				OLFPVOLF			902.5868(1.6)
VOLFPVOLFP	$-CO$	1114.7257	1114.7267(0.9)	FPVOLFPV	$-(CONH + H^\bullet)$	871.5489	871.5446(4.9)
VOLFPVOLFP	$-CH_4N$	1112.6915	1112.6872(3.9)	LFPVOLF	$-H_2O$	813.5014	813.5022(9.8)
VOLFPVOLFP	$-2(H_2O)$	1106.7020	1106.6966(4.9)	VPFLOVP	$[M + H]^+$	767.4735	767.4819(10.9)
VOLFPVOLFP	$-C_3H_6$	1099.6658	1099.6671(11.8)	LFPVOL	$[M + H]^+$	684.4335	684.4448(16.5)
VOLFPVOLFP	$-(C_3H_6 + H^\bullet)$	1098.6671	1098.6592(7.2)	VOLFPV	$[M + H]^+$	670.4308	670.4292(2.4)
	$-C_2H_6N$		1098.6720(4.1)				
VOLFPVOLFP	$-C_4H_8$	1086.6600	1086.6590(1.0)	LFPVOL	$-H_2O$	666.4348	666.4338(1.5)
VOLFPVOLFP	$-(C_4H_8 + H^\bullet)$	1085.6597	1085.6511(7.9)	VOLFP	$-CH_3$	557.3445	557.3457(2.2)
VOLFPVOLFP	$-(C_3H_9N + H^\bullet)$	1082.6451	1082.6403(4.4)	VOLFP	$-NH_3$	556.3488	556.346(5.1)
VOLFPVOLFP	$-(C_2H_6N + NH_3)$	1081.6567	1081.6451(10.7)	LFVP	$[M + H]^+$	457.2811	457.2815(0.9)
VOLFPVOLFP	$-(C_3H_7N + NH_3)$	1068.6455	1068.6373(7.7)	VOLF	$-2 \times NH_3$	442.2819	442.2707(25.3)
VOLFPVOLFP	$-(C_3H_9N + H_2O + H^\bullet)$	1064.6233	1064.6298(6.1)	OLFP	$-(CONH + H^\bullet)$	429.2873	429.2866(1.6)
VOLFPVOLFP	$-(C_2H_4NH_2 + C_3H_6)$	1056.6215	1056.6247(3.0)	LFP	$-(CONH + H^\bullet)$	315.2064	315.2073(2.9)
VOLFPVOLFP	$-C_7H_8$	1050.6512	1050.6589(7.3)	OVP	$[M + H]^+$	311.2080	311.2083(1.0)
VOLFPVOLFP	$-(C_3H_9N + C_3H_6 - H_2 + H^\bullet)$	1043.6109	1043.6131(2.1)	OLF	$-C_6H_5$	297.1922	297.1928(2.0)
				OVP	$-CH_4$		297.1932(3.3)
VOLFPVOLFP	$-(C_3H_7N + C_3H_6)$	1042.6083	1042.6090(0.7)	LF	immonium ion	233.1649	233.1654(2.1)
VOLFPVOLFP	$-(C_3H_7N + C_4H_8)$	1029.6019	1029.6011(6.8)	VP	$[M + H]^+$	197.1286	197.1289(20.3)
VOLFPVOLFP	$-(C_3H_7N + C_4H_8 + H^\bullet)$	1028.6024	1028.5933(8.8)	VP	immonium ion	169.1336	169.1341(3.0)
VOLFPVOLFP	$-(C_3H_7N + C_3H_6 + H_2O)$	1025.6016	1025.6059(4.1)	F	immonium ion	120.0807	120.0813(5.0)
LFPVOLFPV	$-CH_3$	1013.6162	1013.6193(3.1)	O	$[M + H]^+$	115.0866	115.0871(4.3)

[a] Masses are calculated as described in the text, mass errors (in ppm) between calculated and measured masses are noted in parentheses, and fragments are expressed relative to $[M + 2H]^{+\bullet}$. Note: Because these are cyclopeptides, masses are calculated as the sum of the amino acid residue masses (without the usual endgroups) minus the fragment.

Amplification of Side-Chain Cleavages. The initial assumption, that ECD would amplify the detection of side-chain cleavages, is well borne out by the spectra presented in Figure 1. In each case, the side-chain cleavages are abundant, and the relative abundances of fragment ions resulting from backbone cleavages are reduced as compared to ECD of linear peptides.[9] Although side-chain losses have been reported before,[9,19,20,34] the side-chain losses of $CH_3^\bullet$, $C_3H_7^\bullet$, phenylalanine, the radical form of histidine, and the loss of the novel amino acid side chains of cyclosporin *A* have not previously been reported. These new losses, in combination with the previously reported side-chain cleavages, confirm that side-chain fragmentation of peptides is facile with ECD.

Multiple Backbone Cleavages. Although $H^\bullet$ losses and side-chain cleavages are frequent, multiple backbone bond cleavages are required to explain the majority of the peaks present in Figure 1. These multiple backbone cleavages require that one electron capture event results in more than one bond cleavage so that secondary fragmentation (presumably radical mediated) is not only present, but is extremely common. Furthermore, the prevalence of mass losses corresponding to individual or adjacent amino acid residues requires fragmentation of two bonds of the same type on either side of the eliminated segment. It is generally difficult with internal fragments to determine whether they are cleaved at $N-C_\alpha$ bonds, $C_\alpha-CO$ bonds, or $CO-NH$ bonds. Prior ECD data,[9,22,24] as well as the solution phase protein radical chemistry literature,[2−4] suggests that the $N-C_\alpha$ bond is the most labile under free radical rearrangements, because of the combination of the relative weakness of the $H-C_\alpha$ bond, the ability to conjugate the α-carbon radical with the carbonyl, and the improved stability of secondary carbon radicals over primary carbon radicals.[5−7] In the cyclosporin *A* spectrum, because of the existence of partial N-methylation, several peaks are observed (such as the *m*/*z* 269.1865 peak which corresponds to $[mCyB + H]^+$) which can only be formed by cleavage of the $N-C_\alpha$ bond on both sides of the eliminated peptide. The preferential cleavage of the $N-C_\alpha$ bond is also supported by the common loss of CONH (see below) and $CONCH_3$ (for cyclosporin *A*).

Coulombic Potential Energy Release. In general, multiple bond cleavages require more energy for fragmentation than do single bond cleavages so that it is useful to consider, at least qualitatively, possible sources of extra fragmentation energy in ECD of cyclic peptides. Electron capture dissociation reacts a multiply charged precursor ion with low energy electrons, and, provided that the n^+ charge state of the ion captures $<n$ electrons, some of the remaining fragments will be charged and, therefore, detectable by mass spectrometry. However, a multiply charged precursor ion is strained by the Coulombic repulsion of the charges. If an electron is captured by a doubly charged peptide and cleaves the backbone $N-C_\alpha$ bond, the Coulombic repulsion potential energy is released and is randomized among the vibrational energy modes of the two fragment species and can be dissipated as a recoil kinetic energy. If the peptide is cyclic, the kinetic energy dissipation mode is not available so that the Coulombic repulsion potential energy is forced exclusively into the (ro-)vibrational modes of the fragment. While it is rare that the position of the two charges is known exactly, the doubly charged ion of gramicidin *S* has been extensively modeled,[35,36] and it has been determined that that the two charges are spaced ∼9.5 Å apart, which yields ∼3.0 eV of

(34) Haselmann, K. F.; Budnik, B. A.; Kjeldsen, F.; Polfer, N. C.; Zubarev, R. A. Can the $(M^\bullet-X)$ region in electron capture dissociation provide reliable information on the amino acid composition of polypeptides? *Eur. J. Mass Spectrom.* **2002**.

Table 4. Cyclosporin *A* $[M + 2H]^{2+}$ ECD Fragment Table[a]

base	fragment	measured masses	calculated masses	base	fragment	measured masses	calculated masses
mVmCyBmGmLVmLAAmLmL	$[M + 2H]^{+\bullet}$	1203.8574	1203.8569(0.4)		unidentified	908.6960	
mVmCyBmGmLVmLAAmLmL	$[M + H]^+$	1202.8486	1202.8491(0.4)	BmGmLVmLAAmLmL	$[M + H]^+$	906.6404	906.6391(1.3)
mVmCyBmGmLVmLAAmLmL	$-H_2O + H^\bullet$	1184.8364	1184.8381(1.4)		unidentified	866.6107	
mVmCyBmGmLVmLAAmLmL	$-(C_4H_7O + H^\bullet) + C_4H_7O$	1132.8116	1132.8072(3.8)		unidentified	852.6310	
mVmCyBmGmLVmLAAmLmL	$-(C_4H_7O + H^\bullet) + C_4H_8$	1076.7466	1076.7446(1.9)	mGmLVmLAAmLmL	$[M + H]^+$	821.5885	821.5864(2.6)
mCyBmGmLVmLAAmLmL	$-(H_2O + H^\bullet)$	1071.7648	1071.7540(10.0)	mLAAmLmLmVmCy	$[M + H]^+$	820.5821	820.5911(11.0)
	unidentified	1064.7389		mCyBmGmLVmLAA	$-(H_2O + H^\bullet)$	817.5519	817.5546(3.3)
mVmCyBmGmLVmLAAmLmL	$-(C_7H_{12}O + C_2H_4)$	1063.7375	1063.7368(0.7)	mVmCyBmGmLVmL mLAAmLmLmVmCy	$[M + H]^+ -(CH_3)$	806.5783	806.5755(3.5) 806.5761(2.7)
mGmLVmLAAmLmLmVmCy	$-(CONCH_3)$	1061.7816	1061.7828(1.1)		unidentified	804.5242	
mVmCyBmGmLVmLAAmL	$-(H_2O)$	1058.7378	1058.7462(7.9)		unidentified	796.5676	
mVmCyBmGmLVmLAAmL	$-(CO + H^\bullet)$	1047.7464	1047.7545(7.7)		unidentified	710.5195	
mVmCyBmGmLVmLAAmLmL	$-(C_7H_{12}O + C_2H_4 + H_2O)$	1045.7263	1045.7258(0.4)		unidentified	662.4502	
	unidentified	1036.7125		mLAAmLmLmV	$[M + H]^+$	637.4658	637.4652(0.9)
BmGmLVmLAAmLmLmV	$[M + H]^+$	1019.7271	1019.7232(3.8)	BmGmLVmLA	$-(CH_3 + H^\bullet)$	566.3803	566.3797(1.1)
mCyBmGmLVmLAAmLmL	$-(C_4H_7O + H^\bullet)$		1019.7231(3.9)	mCyBmGmLVmL	$-(C_4H_7O + H^\bullet) + C_4H_8 + H^\bullet$		566.3791(2.1)
mVmCyBmGmLVmLAAmL	$(C_4H_7O) -(CONCH_3)$		1019.7359(8.6)				
BmGmLVmLAAmLmLmV	$-(CNH)$	993.7121	993.7202(8.1)	mLAAmLmL mGmLVmLAA	$[M + H]^+ -(CONH + H^\bullet)$	524.3800	524.3811(2.1) 524.3812(2.3)
	unidentified	979.6915		mLVmLA AmLmLmV	$[M + H]^+ -(CH_3)$	425.3139	425.3127(2.8) 425.3133(1.2)
mCyBmGmLVmLAAmL	$[M + H]^+$	962.6667	962.6653(1.5)	mLAAmL mCyBmGmL	$[M + H]^+$	397.2819	397.2814(1.3)
mLAAmLmLmVmCyBmL	$-(CH_3)$		962.6659(0.8)		$-(C_4H_7O + H^\bullet) (C_4H_7O)$		397.2814(12.6)
	unidentified	951.6518		mCyB	$[M + H]^+$	269.1865	269.1865(0.0)
mVmCyBmGmLVmLAA	$[M + H]^+$	948.6514	948.6497(3.0)	mLmV mLmL	$[M + H]^+$	241.1915	241.1916(0.4)
mCyBmGmLVmLAAmL	$-(CH_3)$		948.6502(1.3)		$-(CH_3)$		241.1921(2.9)
mCyBmGmLVmLAAmL	$-(H_2O + H^\bullet)$	944.6548	944.6543(0.5)		unidentified	224.1648	
mGmLVmLAAmLmLmV	$[M + H]^+$	934.6726	934.6704(2.2)				
mCyBmGmLVmLAAmL	$-(CO + H^\bullet)$		934.6704(2.4)				

[a] Masses are calculated as described in the text, mass differences between calculated and measured masses are noted in parentheses, and fragments are expressed relative to $[M + 2H]^{+\bullet}$. Note: Because these are cyclopeptides, masses are calculated as the sum of the amino acid residues masses (without the usual endgroups) minus the fragment.

Coulombic repulsion potential energy. Thus, ECD of gramicidin *S* $[M + 2H]^{2+}$ ions results in an additional ~3 eV of Coulombic repulsion energy available for reactions. While the primary electron capture reaction causes an extremely rapid nonergodic dissociation,[9] any excess energy from the ECD reaction in addition to this ~3 eV of Coulombic repulsion energy will be fully randomized into the vibrational modes of the opened ring fragment. Given that the mean internal vibrational energy of molecules of this size is ~2−3 eV at room temperature,[37] this represents roughly a doubling of the internal energy of the molecule.

While a typical backbone amide bond cleavage would require ~4−5 eV of vibrational energy to accumulate in a single bond prior to fragmentation, free radical reactions of peptides proceed via very low energy electron rearrangements,[3,4] which can be exoergodic.[7] Figure 3 demonstrates one rearrangement which will allow a free radical reaction initiated by the expected nonergodic dissociation method to propagate along a peptide backbone. The nonergodic electron capture[9] forms an energetic α-carbon radical as per eq 1. An α-carbon radical can rearrange to shift the radical over to a neighboring residue carbonyl (B → C), cleaving the N−C_α bond and generating yet another α-carbon radical (C → D) which can then continue this reaction.

In addition to shifting the radical along the backbone by losing cyclic neutrals, an α-carbon radical can abstract a hydrogen from another amino acid (Figure 4), thus propagating the radical (and, inversely, the $H^\bullet$) along the protein backbone. Hydrogen abstraction from an α-carbon is a low energy (and sometimes exoergodic) process because one H−C_α bond is formed and one H−C_α bond is cleaved with the protein side chain providing the energetic differences between the stability of the radical at various α-carbon sites throughout the molecule.[7] These abstractions will be governed by the ability of the site to stabilize the radical and by the H-atom affinity of the various sites.[24] These free radical rearrangements, as secondary ECD reactions, will be kinetically limited as the radical site must vibrate into proximity for this radical rearrangement to occur, and it will be constrained by steric hindrance in the peptide. Rearrangements that result in fragmentation are also entropically driven under normal ECD conditions, as the probability of the fragments returning into proximity for a back reaction is essentially zero.

Besides the migration of radicals along the α-carbon positions in the peptide and cleavage of the N−C_α bond, many other free radical rearrangement reactions are possible. Additional free radical reactions that are supported by the spectra shown are noted in Figure 5. Figure 5A involves migration of an $H^\bullet$ to the side chain followed by loss of the side chain and formation of yet another α-carbon radical. Figure 5B is similar, but involves a shift of the radical to the side chain instead of $H^\bullet$. Figure 5C−F proposes mechanisms for the small molecule losses of HCN, H_2O, CONH, and NH_3, respectively. A common feature

(35) Gross, D. S.; Williams, E. R. Structure of gramicidin *S* [M + H + X](2+) ions (X = Li, Na, K) probed by proton-transfer reactions. *J. Am. Chem. Soc.* **1996**, *118*, 202−204.
(36) Gross, D. S.; Williams, E. R. Experimental measurement of Coulomb energy and intrinsic dielectric polarizability of a multiply protonated peptide ion using electrospray ionization Fourier transform mass spectrometry. *J. Am. Chem. Soc.* **1995**, *117*, 883−890.
(37) Drahos, L.; Vekey, K. Determination of the thermal energy and its distribution in peptides. *J. Am. Soc. Mass Spectrom.* **1999**, *10*, 323−328.

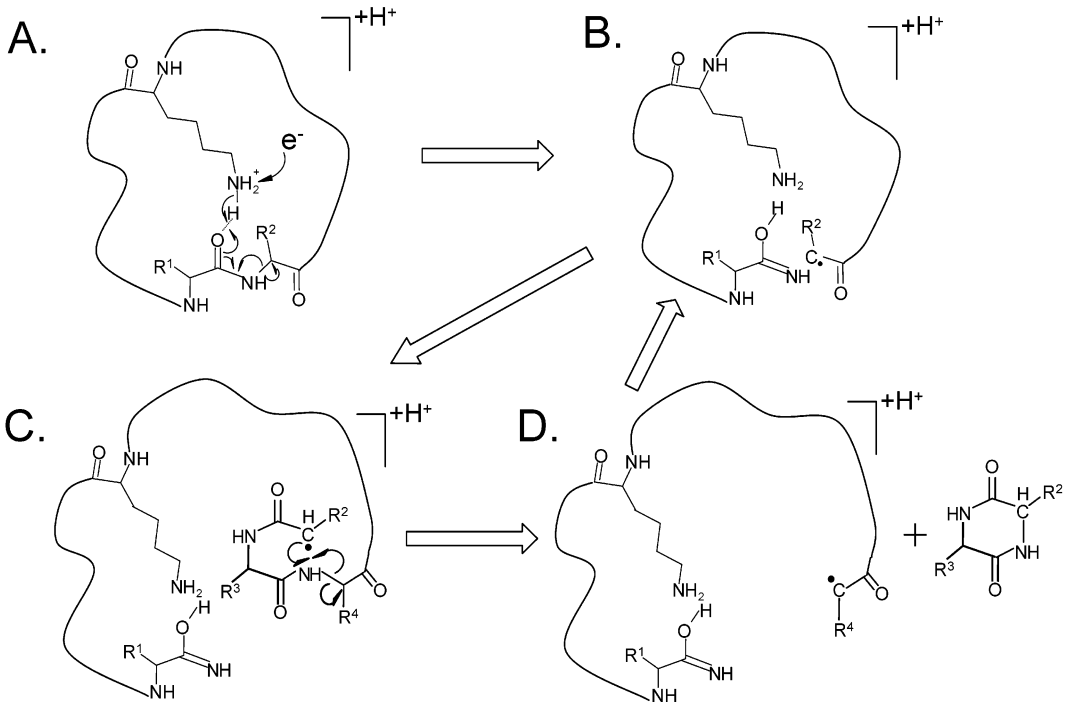

Figure 3. Nonergodic cleavage from electron capture dissociation (A → B) initiates an α-carbon radical which can propagate along a peptide backbone by free radical rearrangements (B → C → D), cleaving the N−C_α bond and forming another α-carbon radical.

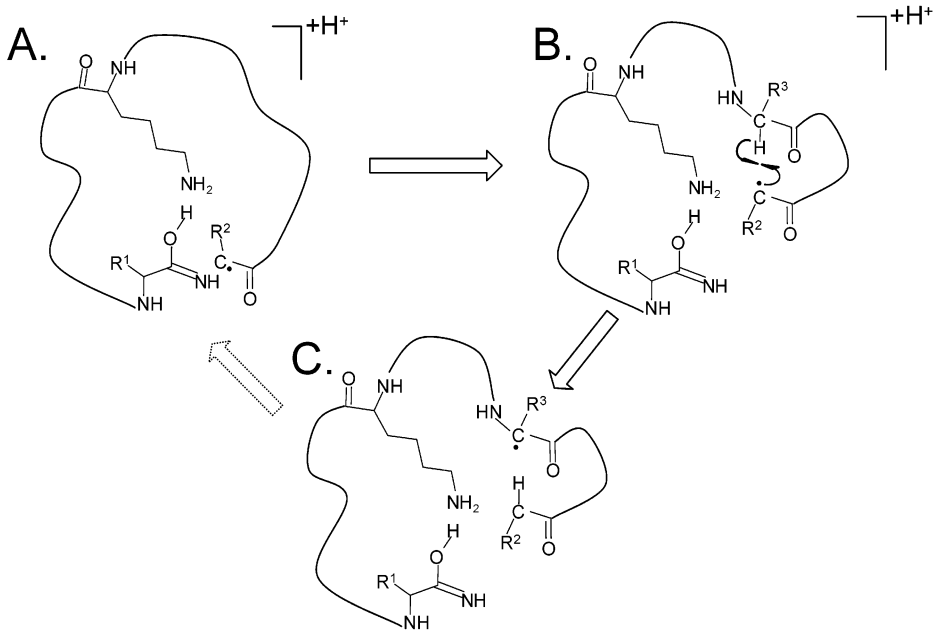

Figure 4. The α-carbon radical can propagate along a peptide backbone by hydrogen abstraction (B → C).

of many of these reactions is that the rearrangement results in the radical position migrating to an α-carbon where it is resonantly stabilized, but where it is also free to participate in further free radical rearrangements of the types illustrated in Figures 3−5.

Glycine. Interestingly, the observed backbone cleavages also show a strong prevalence for the loss of glycine, an amino acid that is not abundant in these peptides. Literature suggests that glycine is slightly preferred in the formation of α-carbon radicals due to lack of side-chain steric interactions which allows the Cα−CO region to achieve planarity, improving resonance stabilization of the radical.[2,38] Additionally, nascent glycine residues are formed as a result of many of the noted side-chain cleavages, a reaction which may be driven by the same considerations.

Stabilized Radical. The spectra above clearly showed that cyclosporin *A* is more able than the other peptides to retain the radical because it shows a prominent $[M + 2H]^{+\bullet}$ ion. This feature can be explained by a spontaneous acid catalyzed rearrangement that has been reported for cyclosporin *A* which

(38) Headlam, H. A.; Mortimer, A.; Easton, C. J.; Davies, M. J. B-scission of the C-3 (*β*-carbon) alkoxyl radicals on peptides and proteins: A novel pathway which results in the formation of α-carbon radicals and the loss of amino acid side chains. *Chem. Res. Toxicol.* **2000**, *13*, 1087−1095.

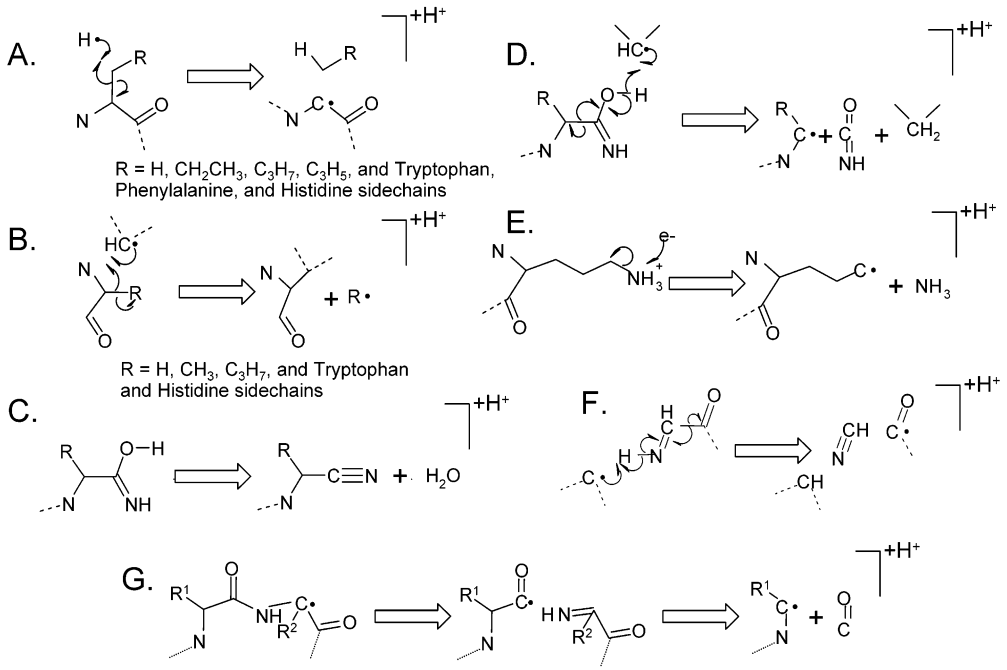

Figure 5. A series of free radical reaction consistent with the spectra shown in Figure 1. (A) Loss of even-electron side-chain fragments by H• transfer, (B) loss of radical side-chain fragments by radical rearrangement, (C) loss of H_2O by radical rearrangement, (D) loss of OCNH by radical rearrangement, (E) loss of NH_3 from residues containing primary amines, (F) loss of HCN by hydrogen abstraction, and (G) cleavage of the amide bond followed by loss of CO by radical rearrangement.

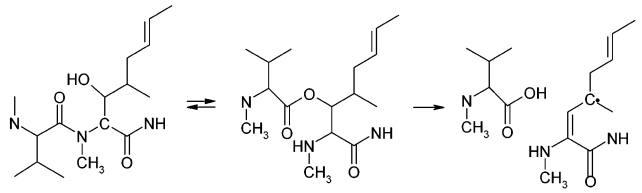

Figure 6. The reported N- to O-acyl shift in cyclosporin both creates a position that is highly vulnerable to McLafferty rearrangements and resonantly stabilizes a tertiary carbon radical.

forms an ester bond to the MeCya side chain (Figure 6).[39] This species is highly vulnerable to a McLafferty rearrangement and is driven in this direction by the added resonant stability of the products. This product species forms a particularly stable tertiary carbon radical site (marked with a •) that is resonantly stabilized in the isocyclosporin form. Although full exploration of the cyclosporin *A* isomerization is beyond the scope of this work, consideration of this rearrangement allowed assignment of one additional fragment, but the full implications of the additional isomer are not yet clear. Stabilized molecular radical cations of peptides have been previously noted in the literature as well.[40]

The mobile H• mechanism[24,25] is supported by these data (for example, Figure 5A), and migration of the radical position along the α-carbons of the backbone (Figure 4) provides a mechanism which explains the observed H• mobility. The crucial point is that the existence of the radical requires that there be one incomplete bond, which is best stabilized on an α-carbon, but the thermodynamic difference in energy among the various α-carbon positions is low. This mechanism, therefore, predicts that a peptide, partially deuterated at the α-carbons, will experience scrambling of these deuterium atoms. Prior data showed that the site of cleavage in ECD was correlated with the site's hydrogen atom affinity, with disulfide bonds being a full 1 eV greater than the backbone carbonyl.[24] Thus, the hydrogen atom affinity of the disulfide bond gives us an additional prediction that ECD of a fully α-carbon deuterated peptide that has at least one disulfide bond will transfer a deuterium to the disulfide bond rather than a hydrogen atom originating from somewhere else in the peptide. Both of these predictions can be tested by tandem mass spectrometry.

The observation that one electron capture initiates the cleavage of several bonds suggests that, while the primary fragmentation can be explained by the nonergodic dissociation mechanism,[9] the secondary (and higher order) fragments can be caused by free radical rearrangements of this type. However, in addition to the radical migrations, additional mechanisms involving attack of the radical site are also apparent, and it appears that H• migration may actually be a special case of a radical site attack in which the radical attacks the protein backbone and abstracts a hydrogen atom. Additionally, the frequent loss of CONH from small oligopeptides implies preferential cleavage of the N−C_α bond by both the nonergodic dissociation and the radical migration mechanisms. A mechanism involving a cascade of free radical rearrangements both incorporates the prior knowledge and appears to be a more general statement of the mechanism of formation of ECD reaction products.

Thus, the primary nonergodic ECD reaction occurs on a picosecond time scale and creates a radical site. This radical site then initiates a cascade of radical rearrangement reactions (occurring on a slow, microsecond time scale), such as those in Figures 3−5, which continue until one of the following happens: (1) The radical departs (e.g., H• loss or His• loss). (2) The various energy losses incurred during these rearrangements

(39) Jegorov, A.; Havilcek, V. Spontaneous N−O acyl shift in the $[M + H]^+$ ions of [mebmt]-cyclosporins in an ion trap. *J. Mass Spectrom.* **2001**, *36*, 633−640.

(40) Chu, I. K.; Rodriquez, C. F.; Lau, T.-C.; Hopkinson, A. C.; Siu, K. W. M. Molecular radical cations of oligopeptides. *J. Phys. Chem. B* **2000**, *104*, 3393−3397.

cool the ion sufficiently that further rearrangements become slow on the time scale of the measurement (seconds). (3) The radical is stabilized in a position of low reactivity, for example, in a site where resonance stabilization is strong (note that (2) involves kinetic limitation of the reaction, while (3) involves thermodynamically trapping the radical).

This hypothesis appears to be fully consistent with all previously published ECD spectra, explains the formation of the highly nonspecific *c*/*z*• ions, and easily explains the persistent ±1 Da differences that frequently occur in ECD spectra, as these simply involve either H_2 losses or the presence/loss of H•. Furthermore, as Zubarev et al.[9] noted, for collisionally activated dissociation (MS^3) of the charge reduced $[M + 8H]^{7+\bullet}$ ubiquitin molecular ion, the fragments observed were the *c*/*z*• series rather than the *b*/*y* series expected for CAD, and the ECD/CAD spectrum showed more coverage than the ECD spectrum alone. Zubarev et al.[9] explained the results as cleavage of the backbone without cleavage of the noncovalent (e.g., hydrogen) bonds that held the complex together, and cleavage of the protein backbone without cleaving noncovalent bonds has been verified by several groups[41−43] even to the point of being used to propose specific gas-phase protein structures.[44] However, as an alternative explanation, this result is perfectly consistent with the above hypothesis, as the free radical reaction cascade was prohibited from continuing in the charge reduced species, either by noncovalent bonds and steric interactions keeping the α-carbon radical away from reactive sites or by a lack of energy to rearrange into a reactive geometry. Addition of energy from collisions with background gas reinitiated the radical reaction cascade and allowed it to continue. The difference between the two mechanisms is 1.0078 Da depending on whether the H• or radical site is still contained within the complex. Measuring this difference in the presence of the isotopic distribution will be difficult, particularly if both the $[M + 8H]^{7+\bullet}$ and the $[M + 7H]^{7+}$ species are simultaneously present, as has been confirmed experimentally.[31]

One particularly interesting case, where both H• migration and radical rearrangement are potentially visible, is the disulfide bond. Zubarev et al.[24] have noted the preference of cleavage at disulfide bonds with ECD and postulated a radical rearrangement from the α-carbon to the R−S−S−R moiety (ref 20, eq 5) forming a disulfide radical (RS•) and a cyclized peptide, while Rauk et al.[5] have calculated that the sulfide radical (RS•) will abstract an H• from an α-carbon, shifting the radical to back to the α-carbon, and that this reaction is exoergodic by ∼0.5 eV. Therefore, provided sufficient energy is available for the radical to move into proximity with the disulfide bond, the disulfide bond will cleave and then transfer the radical to yet another α-carbon.

N−C_α versus Amide Bond. In Figure 3, the rearrangement of the radical from the α-carbon to a neighboring residue cleaves the N−C_α bond, and these mass spectra reinforce the observed trend for cleavage of this bond.[9] Additionally, a low abundance loss of CO and HCN is observed in these spectra, Figure 4F and G, and involves cleavage of the amide bond. The CO loss can be explained by a mechanism that is similar to the lower abundance fragmentation channel of ECD which is responsible for formation of the *a*•/*y* ion series.[9] One significant difference in this mechanism is that it does not involve transfer of H•, instead involving an electronic rearrangement that shifts the radical. Nevertheless, this forms a relatively unstable carbonyl radical and thus would be expected to lose CO, a prediction that appears to be confirmed by the spectra, albeit infrequently. Much more common is the loss of CONH (or for cyclosporin *A*, $CONCH_3$), which requires cleavage of the N−C_α bond and the CO−C_α bonds.

Conclusions

For small cyclic peptides, one electron capture by the $[M + 2H]^{2+}$ ion causes multiple backbone cleavages and increases the relative abundance of side-chain cleavages. Although the side-chain cleavages are expected, the multiple backbone cleavages can best be explained by a mechanism in which electron capture induces nonergodic cleavage and generates an α-carbon radical species. This radical then propagates along the protein backbone and initiates multiple free radical rearrangements that cause both secondary backbone cleavages and additional side-chain cleavages.

Acknowledgment. The authors wish to thank Mark McComb for helpful discussions. The work was supported by NIH P41-RR10888 (P.I. C. Costello), NIH P0168705 (P.I. M. Skinner), and The Gerry Foundation (P.I. M. Skinner).

JA028831N

(41) Haselmann, K. F.; Jorgensen, T. J. D.; Budnik, B. A.; Jensen, F.; Zubarev, R. A. Electron capture dissociation of weakly bound polypeptide polycationic complexes. *Rapid Commun. Mass Spectrom.* **2002**, *16*, 2260−2265.
(42) Haselmann, K. F.; Budnik, B. A.; Olsen, J. V.; Nielsen, M. L.; Reis, C. A.; Clausen, H.; Johnsen, A. H.; Zubarev, R. A. Advantages of external accumulation for electron capture dissociation in Fourier transform mass spectrometry. *Anal. Chem.* **2001**, *73*, 2998−3005.
(43) Breuker, K.; Oh, H.; Horn, D. M.; Cerda, B. A.; McLafferty, F. W. Detailed unfolding and folding of gaseous ubiquitin ions characterized by electron capture dissociation. *J. Am. Chem. Soc.* **2002**, *124*, 6407−6420.
(44) Oh, H.; Breuker, K.; Sze, S. K.; Ge, Y.; Carpenter, B. K.; McLafferty, F. W. Secondary and tertiary structures of gaseous protein ions characterized by electron capture dissociation mass spectrometry and photofragment spectroscopy. *Proc. Natl. Acad. Sci. U.S.A.* **2002**, *99*, 15863−15868.